

PIV measurements of a shock-accelerated fluid instability

Katherine Prestridge^a, Peter Vorobieff^b, Paul M. Rightley^a
and Robert F. Benjamin^a

^aDynamic Experimentation Division, Los Alamos National Laboratory, Los Alamos, USA

^bDepartment of Mechanical Engineering, University of New Mexico, Albuquerque, USA

ABSTRACT

A varicose-profile, thin layer of heavy gas (SF_6) in lighter gas (air) is impulsively accelerated by a planar, Mach 1.2 shock, producing Richtmyer-Meshkov instability. We present the first measurements of the circulation in the curtain during the vortex-dominated, nonlinear stage of the instability evolution. These measurements, based on particle image velocimetry data, are employed to validate an idealized model of the nonlinear perturbation growth.

Keywords: Richtmyer-Meshkov, shock, instability, fluid, particle image velocimetry

1. INTRODUCTION

In this study, we present experimental measurements of the circulation in a shock-accelerated thin layer of SF_6 gas embedded in air (i.e. gas curtain). With these measurements, we validate an inviscid, point-vortex model of nonlinear gas-curtain instability growth¹ by comparing our results with its predicted parameter, the circulation of the vortex cores. This is the first time that the circulation derived from a simple model of mixing width growth has been compared to a measured value of circulation. This comparison provides the connection among an inviscid model, traditional integral measurements of the mixing-layer width, and detailed velocity-field measurements.

Richtmyer-Meshkov instability (RMI) developing on shock-accelerated, perturbed density interfaces goes through several stages of evolution before eventual transition to turbulence.² The initial, linear growth stage was first theoretically described by Richtmyer.³ Subsequently, the instability grows in a nonlinear manner, and the flow is dominated by the vortices created by the initial baroclinic vorticity generation. Several theoretical models have been developed to describe this nonlinear region of the instability's development.^{1,4-7} Only measurements of large-scale features of the flow have been available to validate those growth models up to now. While our present findings describe the second stage of the curtain evolution (nonlinear, vortex-dominated growth), the same experimental technique applied at later times can produce quantitative information about the transition to turbulence.

We study the development of the interfaces of a perturbed curtain (i.e. thin layer) of heavy gas (SF_6) embedded in ambient air when the curtain is accelerated by a Mach 1.2 normal shock created in a horizontal shock tube. The shock-tube facility is the same as that used in earlier experiments,⁸⁻¹⁰ except for the improved diagnostics. The current experimental configuration will be described in detail elsewhere.¹¹

The test section of the shock tube (75 mm square) is shown in Fig. 1. A laminar curtain of SF_6 is injected through a contoured nozzle vertically into the top side of the test section and removed on the bottom side. The nozzle profile imposes a varicose perturbation with dominant wavelength $\lambda = 6$ mm on the curtain. The SF_6 is seeded with small ($d \leq 0.5 \mu\text{m}$) glycol/water droplets from a theatrical fog generator which allow us to make the particle image velocimetry (PIV) measurements. See Refs.² and¹¹ for detailed analyses which show that the fog particles accurately track the SF_6 curtain. The tube creates high quality planar shocks of Mach 1.2 that propagate through the test section and accelerate the curtain.

The gas curtain is illuminated using two frequency-doubled, pulsed Nd:YAG lasers, the first of which is a customized, burst-mode laser that is configured to fire seven pulses (100-ns duration, 3 mJ) spaced 140 μs apart. The second is a commercial 10 Hz laser (New Wave Research Minilase-20) with a 10-ns, 10-mJ pulse, which is fired once per event. The light from both lasers is focused into coplanar, horizontal sheets in the test section, as shown in Fig. 1, and three single-frame, gated, intensified CCD cameras by Hadland Photonics (model SV-533 BR, 1134 \times 468 pixels) look at fixed, preset fields of view. The "IC" camera records the image of the initial conditions on one

Send correspondence to: E-mail: kpp@lanl.gov

RECEIVED

SEP 2 8 2000

© STI

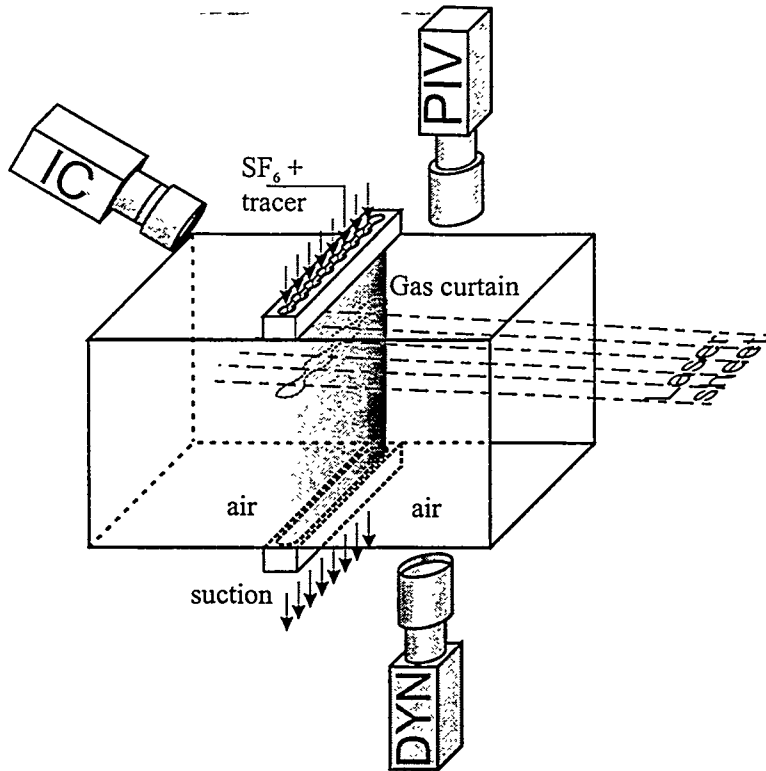


Figure 1. Shock tube test section (shock propagates from left to right).

frame, while the “Dynamic” (“DYN” in Fig. 1) camera observes the rest of the test section to capture multiple exposures of the gas curtain as it is advected downstream. The large freestream velocity causes all of the images to be physically separated on the CCD. The “PIV” camera focuses on a small region of the dynamic field, about 19 by 14 mm, to detect the individual fog droplets.

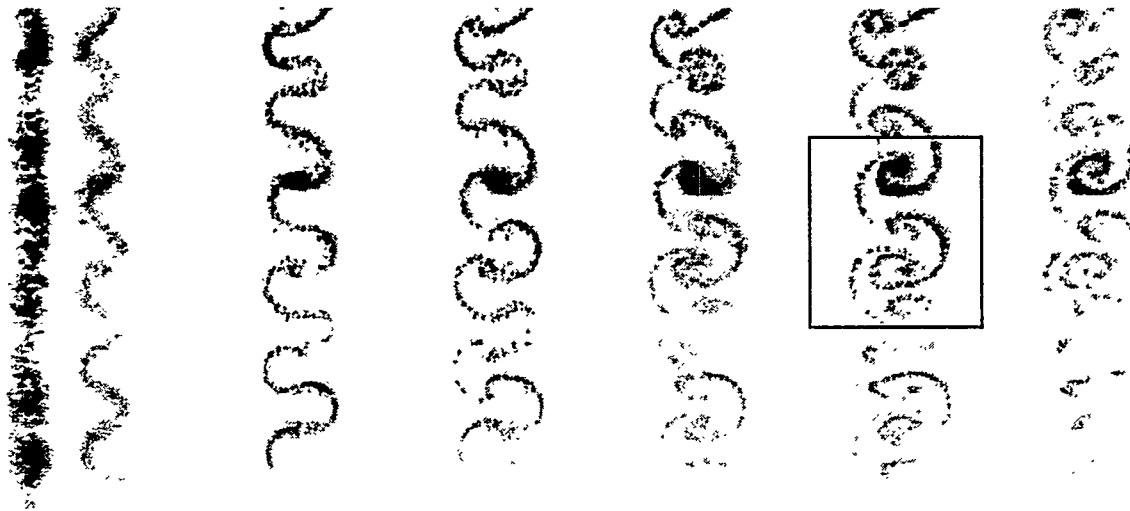


Figure 2. Initial conditions ($t = 0$) and dynamic images at $t = 120, 260, 400, 540, 680$ and $820 \mu\text{s}$ after shock interaction. Region imaged by PIV camera is inside black rectangle.

An image with the view of the initial conditions and the dynamic image from the IC and “Dynamic” cameras is

DISCLAIMER

This report was prepared as an account of work sponsored by an agency of the United States Government. Neither the United States Government nor any agency thereof, nor any of their employees, make any warranty, express or implied, or assumes any legal liability or responsibility for the accuracy, completeness, or usefulness of any information, apparatus, product, or process disclosed, or represents that its use would not infringe privately owned rights. Reference herein to any specific commercial product, process, or service by trade name, trademark, manufacturer, or otherwise does not necessarily constitute or imply its endorsement, recommendation, or favoring by the United States Government or any agency thereof. The views and opinions of authors expressed herein do not necessarily state or reflect those of the United States Government or any agency thereof.

DISCLAIMER

**Portions of this document may be illegible
in electronic image products. Images are
produced from the best available original
document.**

shown in Fig. 2. The actual image from the PIV camera is double-exposed, first from the burst-mode laser at 680 μ s, and then from the single-pulse laser at 698.4 μ s. The latter is not recorded by the “Dynamic” camera because the camera intensifier is gated off during the second pulse.

The negative of the image captured by the PIV camera is shown in Fig. 3a. Visible in the figure is the double exposure caused by the two different laser pulses, separated by 18.4 μ s. We will use the downstream-pointing mushroom structure in the middle of the image to illustrate the process of determining mixing width and circulation in the flowfield. Fig. 3b is the velocity field created by performing single-frame cross-correlation on the image in Fig. 3a. We take the velocity field to be representative of a time midway between the two exposures of Fig. 3a, at 689.2 μ s after shock impact. The measured freestream velocity of 97 m/s has been subtracted from the field. From this

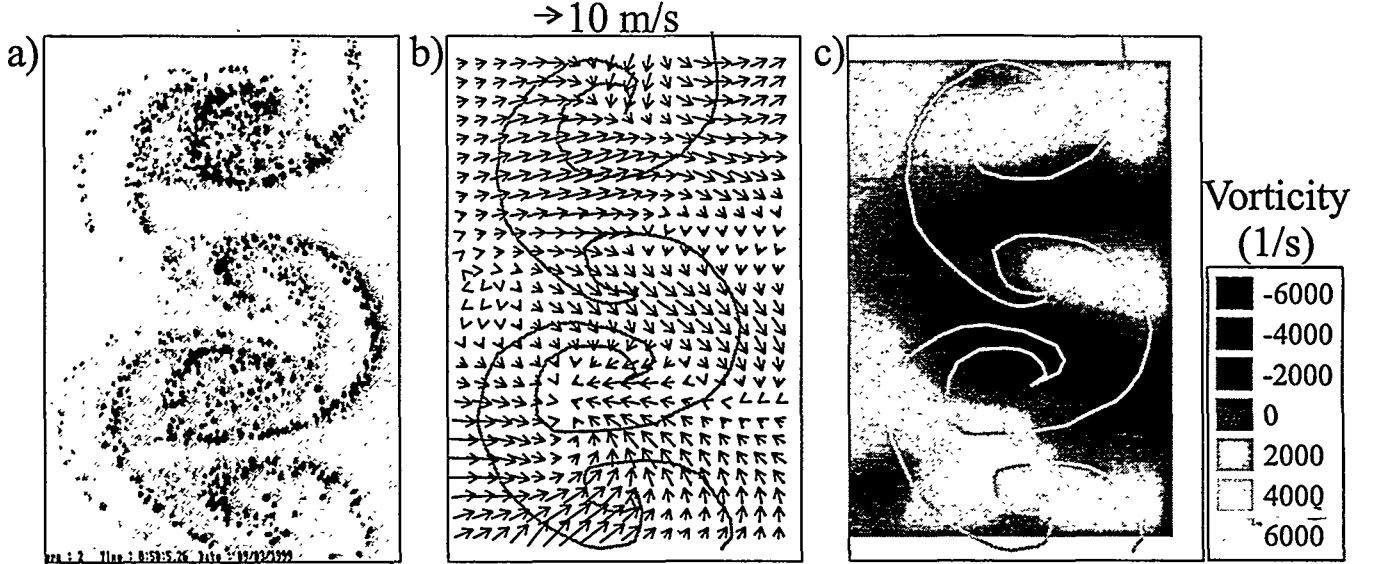


Figure 3. PIV measurements. (a) Region captured by the PIV camera. (b) Velocity field corresponding to the image (a). (c) Vorticity isocontours. The gray line in (b) and (c) shows the position of the curtain midway between the two exposures of (a).

velocity field, a vorticity field is created by calculating the circulation around each vector using the eight surrounding vectors¹²; this is shown in Fig. 3c. What becomes apparent is that each roll-up region at the intersection of the mushroom “stem” and “cap” in Fig. 3a corresponds to a concentration of vorticity, and there is a pair of counter-rotating vortices matching each mushroom. We expect this from observations of the image, and it is confirmed by the PIV measurements. The alternating signs of vorticity caused by the symmetric mushroom structures are clear in the figure.

Using this new flow-field information contained within the large-scale structures, we can now compare the circulation determined from an inviscid growth model with that measured using PIV. Let us first briefly summarize the important features of the model for the growth of the mixing region.^{1,10}

The model is based upon an infinite row of counter-rotating point vortices, approximating the vorticity which is baroclinically generated on the interfaces between the heavy and light gases when the shock impacts the curtain. Each vortex has the same circulation, Γ , and there is one local wavenumber associated with the flow, k , where $k = 2\pi/\lambda$. For the single-mode nozzle used in these experiments, $\lambda = 6$ mm, and k was set at a fixed value of 1.04 mm⁻¹. The expression for the growth of the mixing region in time is^{1,10}:

$$w(t) = \frac{2}{k} \sinh^{-1} \left(k^2 \Gamma (t - t_0) + \sinh \left(\frac{kw_0}{2} \right) \right), \quad (1)$$

where t_0 is the virtual origin and w_0 is the curtain width just after it has been compressed by the shock. This value is estimated to be $w_0 = w_{init}/1.34$, where the measured thickness is divided by the shock compression factor for a Mach 1.2 normal shock. The virtual origin t_0 , absent from the original model,¹ is introduced to account for the phase

inversion of one of the interfaces.^{13,10} Eq. 1 produces a growth rate prediction similar to other nonlinear-growth theories.^{6,7}

Previous analysis quantified the initial thickness and temporal growth of the layer,¹⁰ but the actual circulation of the flow could not be measured. We will continue with the example of Figs. 2 and 3, and illustrate how we measure the growth of the mixing region in the gas curtain and determine the circulation corresponding to the middle mushroom. To preserve the local flow information, we measured the individual widths corresponding to the wavelength along which the center mushroom appeared.

The mixing width evolutions from Fig. 2 for mushrooms A and B are plotted in Fig. 4. It is immediately apparent that the mixing widths corresponding to each mushroom are very similar. Using Γ and t_0 as free parameters, where w_0 and k are fixed parameters measured from the initial conditions, the $w(t)$ data are fit to Eq. 1 (these fits are also shown in Fig. 4). The value k remains nearly constant during instability growth, even though mushroom orientation varies. The model from Eq. 1 converges with a residual, r^2 , of 0.99, where $r^2 = 1.0 - \sum_{i=1}^n [(w_{fit} - w_i)^2 / (w_i - \bar{w})^2]$ and \bar{w} is the average width of the curtain. The curve fit gives us a circulation for the mushroom, such that $\Gamma_{model} = 0.036 \text{ mm}^2/\mu\text{s}$.

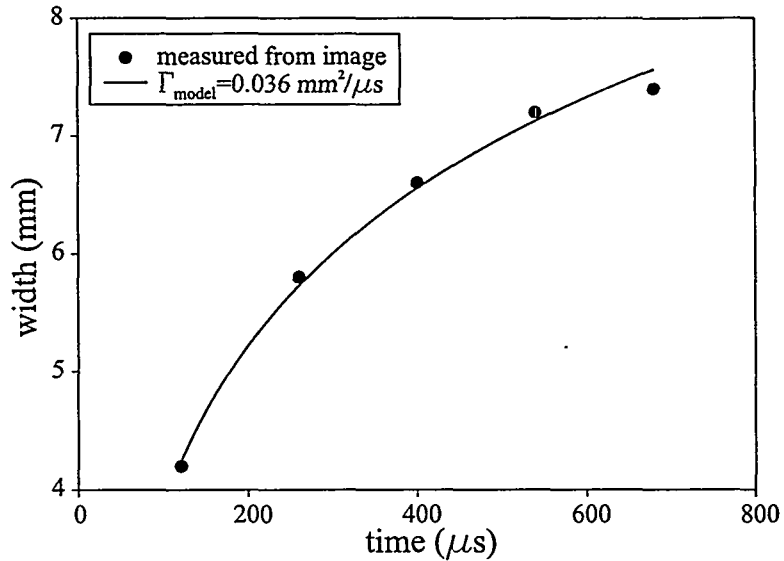


Figure 4. Curve fit using the growth model in Eq. 1. Symbols are experimental data, line is curve fit. Error bars on data points are no larger than the points.

To validate the model in Eq. 1, we compare the circulation from the curve fit of Fig. 4 to the vorticity field of Fig. 3c. The circulation from the PIV data was calculated by drawing a closed curve around the region of negative vorticity corresponding to the middle mushroom and computing the line integral of tangential velocity around the entire curve. This process yields circulation: $\Gamma_{PIV} = 0.035 \text{ mm}^2/\mu\text{s}$. We measured Γ with the curve-fitting and PIV procedures for other data sets, and the comparison between Γ_{PIV} and Γ_{model} is shown in Fig. 5. The range of circulation values from 0.01 to 0.11 $\text{mm}^2/\mu\text{s}$ is caused by uncontrolled but carefully measured variations in the initial state of the varicose interface. The agreement shown in Fig. 5 is quite good, with over two-thirds of the data within an error bar of the fit, $\Gamma_{PIV} = \Gamma_{model}$. Thus, the model (Eq. 1) is a reliable estimator of mixing width during this phase of the instability. It is also noteworthy that the delay, t_0 , recovered by the curve-fit varied from 0 to 60 μs , which is consistent with the duration of the phase inversion observed in our experiments.¹⁴

Several physical effects contribute to observed differences. The model assumes an initially sharp interface, but the actual interface is diffuse.^{10,11} Also, mode-coupling, not included in the model, is beginning at the time of the PIV measurements. For several events in Fig. 5 the counter-rotating vortices are not perfectly aligned in the spanwise direction, as assumed by the model. The correlation of Γ values shown in Fig. 5 is quite good despite these limitations, which suggests that the inviscid vortex dynamics driving the instability are fairly robust, and that dissipation is negligible.

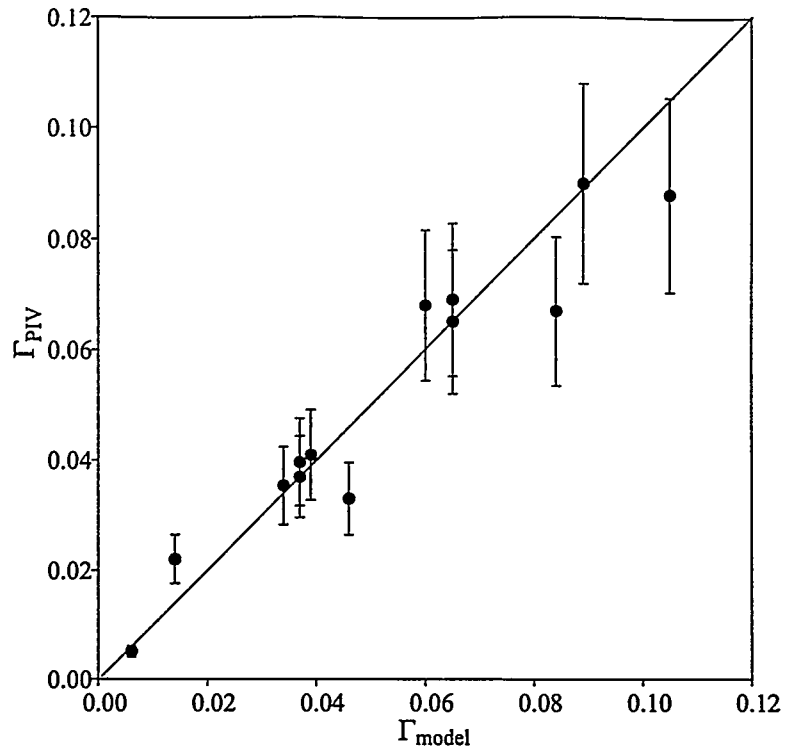


Figure 5. Comparison between the circulation measured using PIV and the circulation from the curve fits of Eq. 1 of mixing width growth for many experiments similar to the one in Fig. 3. Error bars represent PIV measurement uncertainty.

In summary, we have shown that there is agreement between the circulations determined directly from PIV measurements and the circulations deduced from curve fits of the model represented by Eq. 1 to measured mixing width data. Thus, the growth of the curtain with a single, dominant wavelength during the period of nonlinear, vortex-dominated evolution can be modeled using inviscid mechanisms in the regime which we have examined ($t < 1$ ms). Under these flow conditions, there is little apparent dissipation of the initial vorticity deposited in the gas curtain by the shock, as indicated by the close match between the circulation of the idealized model and the circulation calculated from the velocity-field measurements. For the first time, we have been able to make a strong correlation between the circulation predicted from integral measurements of the mix layer and the actual circulation of the large-scale vortex structures within the layer.

ACKNOWLEDGMENTS

This work was supported by DOE contract W-7405-ENG-36 and by Sandia National Laboratories grant BG-7553.

REFERENCES

1. J. W. Jacobs, D. G. Jenkins, D. L. Klein, and R. F. Benjamin, "Nonlinear growth of the shock-accelerated instability of a thin fluid layer," *J. Fluid Mech.* **295**, p. 23, 1995.
2. P. M. Rightley, P. Vorobieff, and R. F. Benjamin, "Experimental observations of the mixing transition in a shock-accelerated gas curtain," *Phys. Fluids* **11**(1), p. 186, 1999.
3. R. D. Richtmyer, "Taylor instability in shock acceleration of compressible fluids," *Commun. Pure Appl. Math.* **23**, p. 297, 1960.
4. R. Samtaney and N. Zabusky, "Circulation deposition on shock-accelerated planar and curved density-stratified interfaces: models and scaling laws," *J. Fluid Mech.* **269**, p. 45, 1994.
5. J. Hecht, U. Alon, and D. Shvarts, "Potential flow models of rayleigh-taylor and richtmyer-meshkov bubble fronts," *Phys. Fluids* **6**, p. 4019, 1994.

6. T. A. Peyser, P. L. Miller, P. E. Stry, K. S. Budil, E. W. Burke, D. A. Wojtowicz, D. L. Griswold, B. A. Hammel, and D. W. Phillion, "Measurement of radiation-driven shock-induced mixing from nonlinear initial perturbations," *Phys. Rev. Lett.* **75**, p. 2332, 1995.
7. Q. Zhang and S. Sohn, "Nonlinear theory of unstable fluid mixing driven by shock wave," *Phys. Fluids* **9**, p. 1106, 1997.
8. J. W. Jacobs, D. L. Klein, D. G. Jenkins, and R. F. Benjamin, "Instability growth patterns of a shock-accelerated thin fluid layer," *Phys. Rev. Lett.* **70**, p. 583, 1993.
9. J. M. Budzinski, R. F. Benjamin, and J. W. Jacobs, "Influence of initial conditions on the flow patterns of a shock-accelerated thin fluid layer," *Phys. Fluids* **6**, p. 3510, 1994.
10. P. M. Rightley, P. Vorobieff, and R. F. Benjamin, "Evolution of a shock-accelerated thin fluid layer," *Phys. Fluids* **9**(6), pp. 1770-1782, 1997.
11. K. Prestridge, P. M. Rightley, P. Vorobieff, and R. F. Benjamin, "Simultaneous density-field visualization and PIV of a shock-accelerated gas curtain," *Exp. in Fluids* , 2000.
12. AEA Technology, Oxfordshire, UK, *VISIFLOW System User Manual*, 1997.
13. Y. Yang, Q. Zhang, and D. H. Sharp, "Small amplitude theory of richtmyer-meshkov instability," *Phys. Fluids* **6**, p. 1856, 1994.
14. P. Vorobieff, P. M. Rightley, and R. F. Benjamin *Proc. 6th IWPCTM Workshop, Marseilles* , p. to be published, June 1997.

24th ICHSPP 25-29 September 2000, Sendai Japan

Particle Image Velocimetry (PIV) measurements of a shock-accelerated fluid instability

Presented by: Dennis Paisley

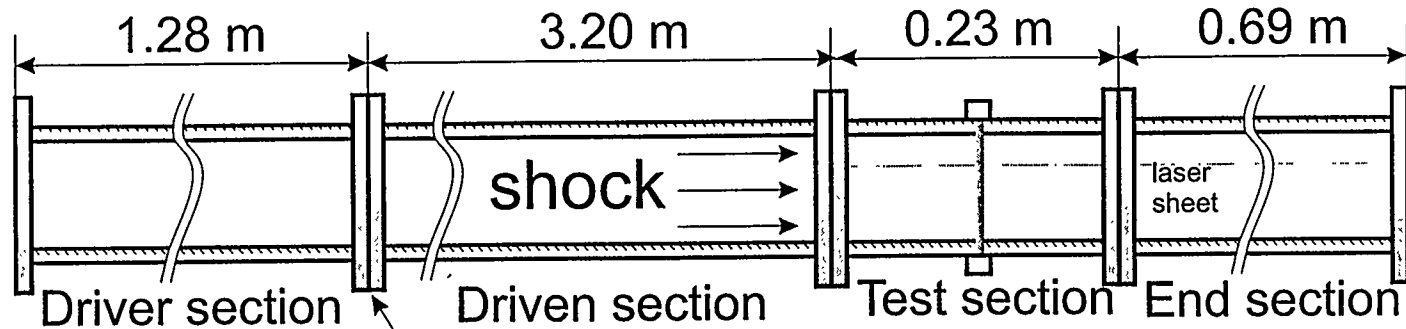
Authors:

Kathy Prestridge (kpp@lanl.gov)
Peter Vorobieff, U. of New Mexico
Paul M. Rightley
Robert F. Benjamin

Dynamic Experimentation Division

Los Alamos
NATIONAL LABORATORY

Gas Shock Tube



Mach Number = 1.2

Gas Curtain:

SF_6 seeded with glycol droplets

2 Lasers:

Customized, doubled Nd:YAG

10 Hz New Wave @532 nm

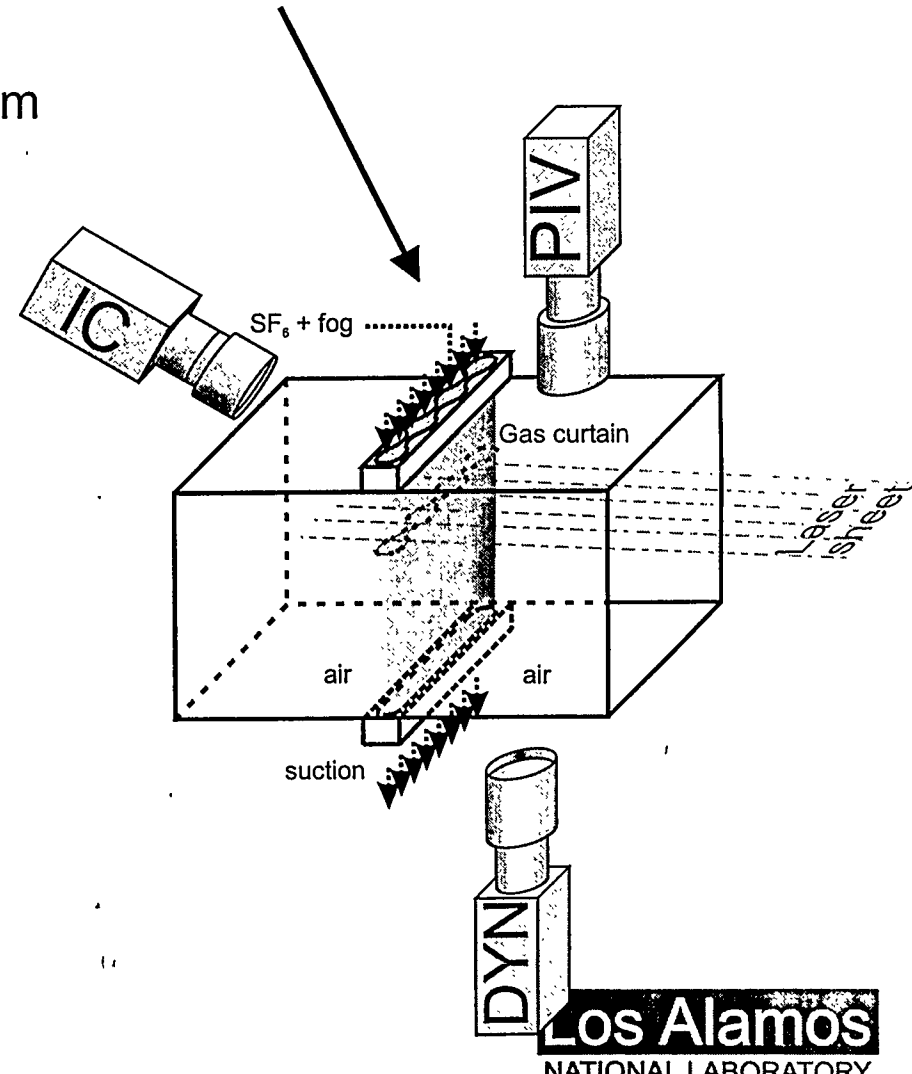
Pulse train:

7 pulses with $\Delta t = 140 \mu\text{s}$

8th pulse for PIV

3 Cameras:

Intensified CCDs, 1134x468



Hadland SV-533 BR Intensified CCD Cameras

Effective resolution: 1134x468 pixels

Generation II Intensifiers (MCP) with 30 line pairs across 40 mm

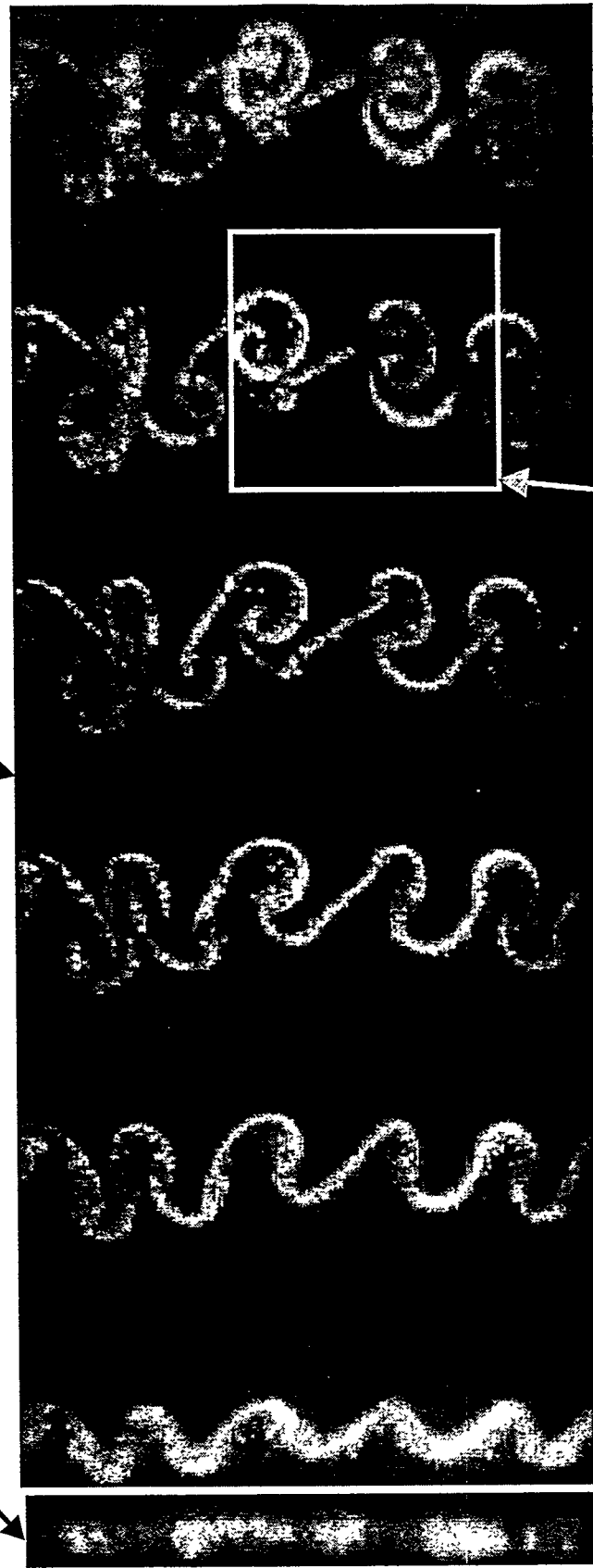
Intensifier is optically coupled to the 8.8 x 6.6 mm CCD chip
using a 28/105 mm lens

Pulsed lasers are used to produce the "frozen" images of the
gas curtain, and the camera's intensifiers are gated open for
10 μ s during each pulse and then closed to eliminate
integration of any stray light

The Richtmyer-Meshkov Instability

Initial Conditions

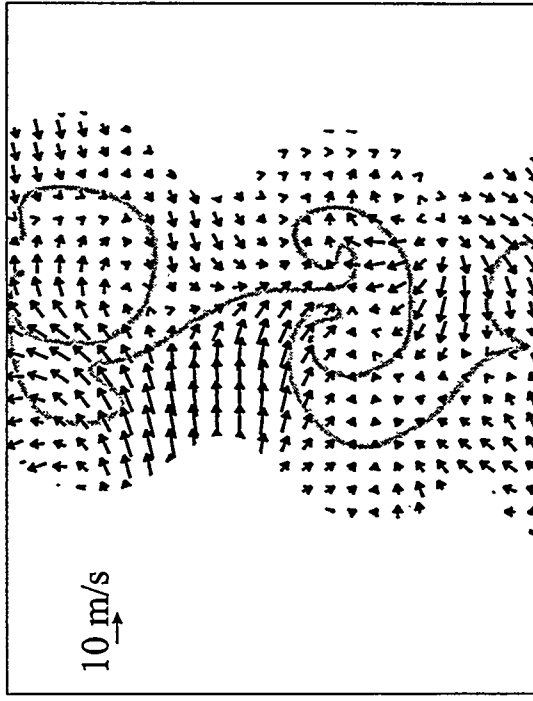
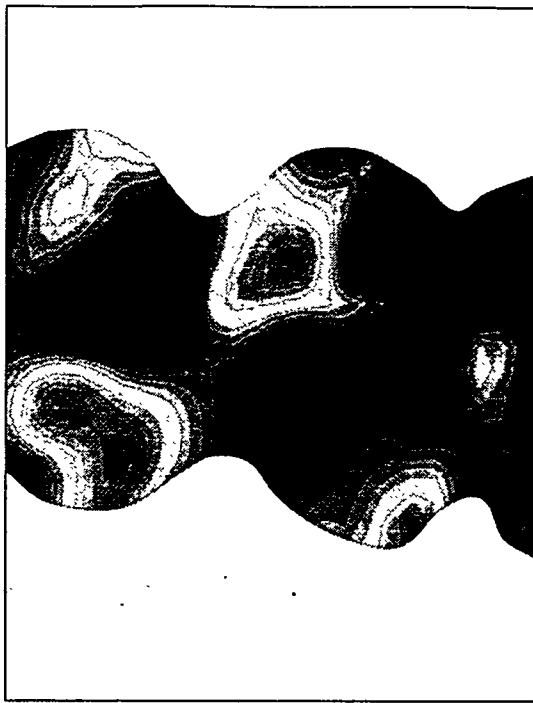
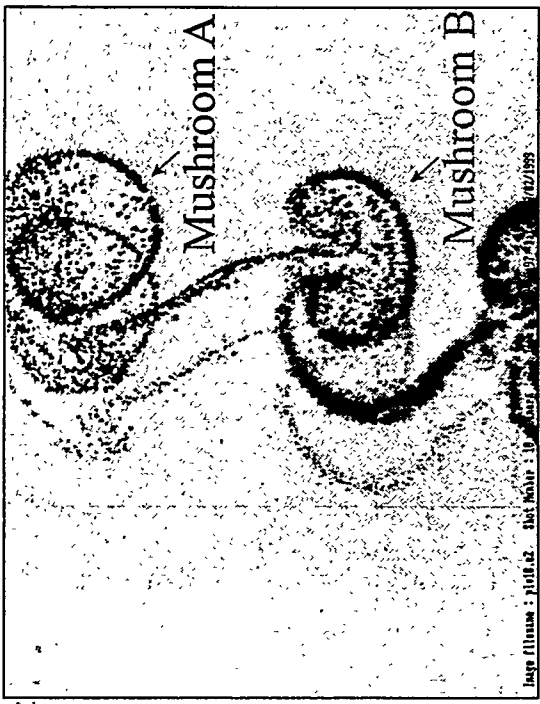
Dynamic Image



PIV field of view

Dynamic Experimentation Division

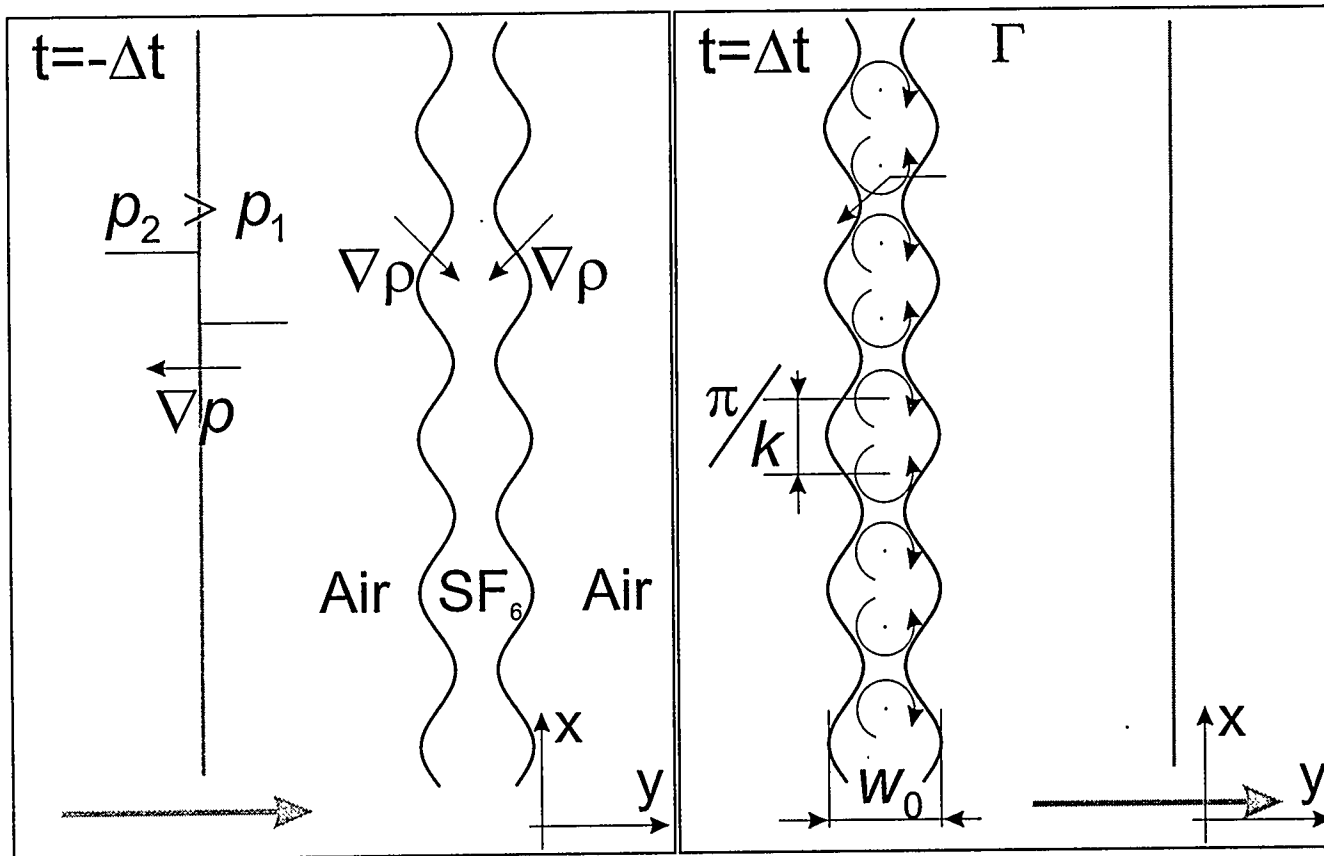
Los Alamos
NATIONAL LABORATORY



Dynamic Experimentation Division

Los Alamos
NATIONAL LABORATORY

Inviscid Model of Instability Growth



Vorticity generation equation has the form:

$$\frac{D}{Dt} \left(\frac{\omega}{\rho} \right) = \frac{1}{\rho^3} \nabla \rho \times \nabla p$$

Assume that the vorticity distribution generated by the interaction of the shock wave with the varicose layer of heavy gas can be approximated by a row of vortices with alternating sign of vorticity.

For a row of line vortices, the stream function will have the form:

$$\Psi = \frac{\Gamma}{4\pi} \ln \frac{\cosh(ky) + \sin(kx)}{\cosh(ky) - \sin(kx)}$$

By direct integration of the equation for the horizontal component of velocity on the interface, the width of the mixing layer can be obtained:

$$w(t) = \frac{2}{k} \sinh^{-1} \left[k^2 \Gamma (t - t_0) + \sinh \left(\frac{kw_0}{2} \right) \right]$$

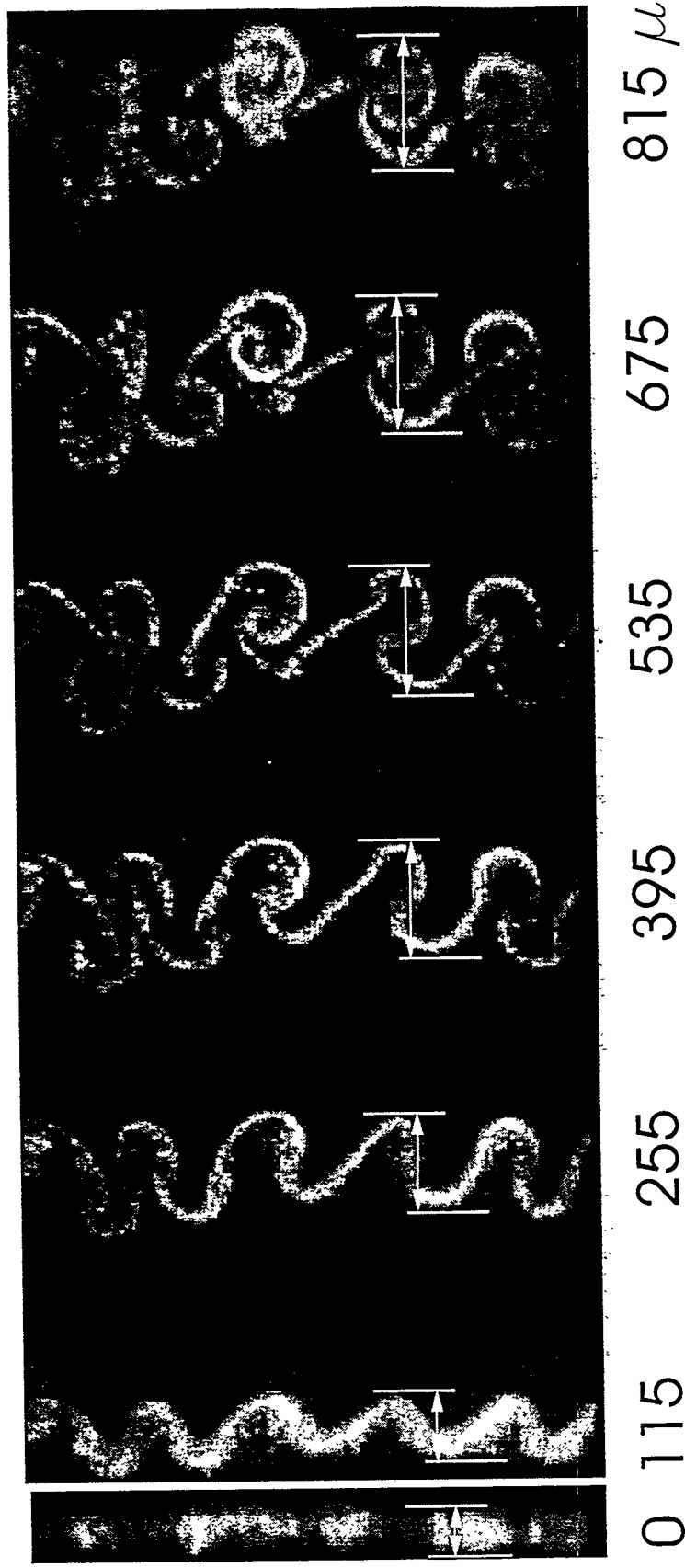
w_0 = initial compressed thickness

$k = 2\pi/\lambda$ = local wavenumber

t_0 = virtual origin

Γ = circulation

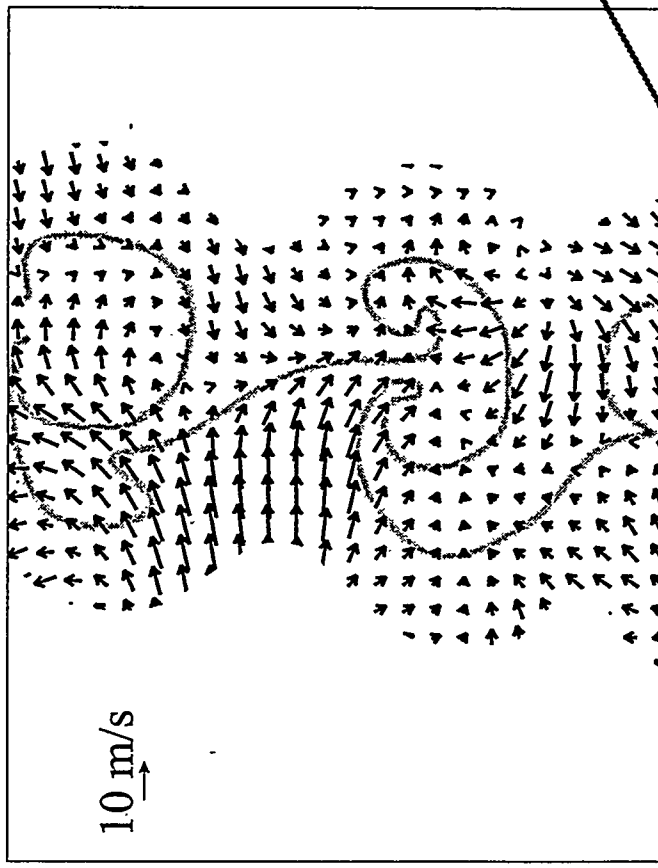
Measuring Curtain Width vs Time



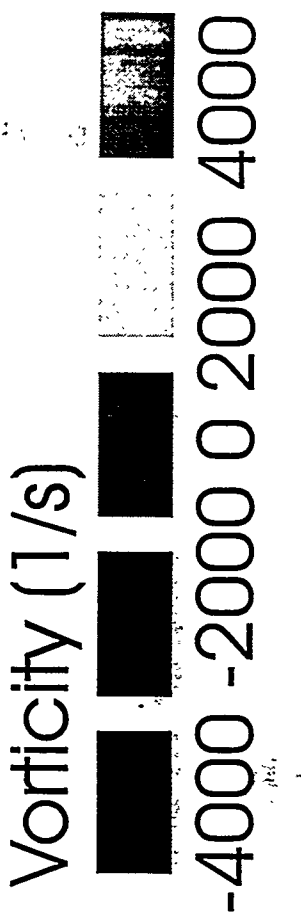
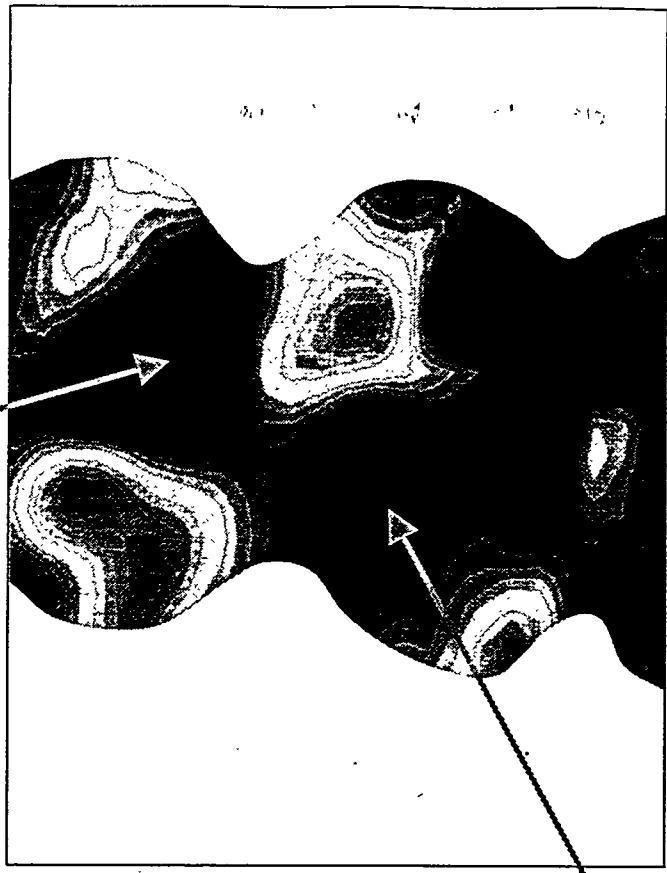
Use measurements to predict circulation using inviscid model

Measure circulation directly using PIV

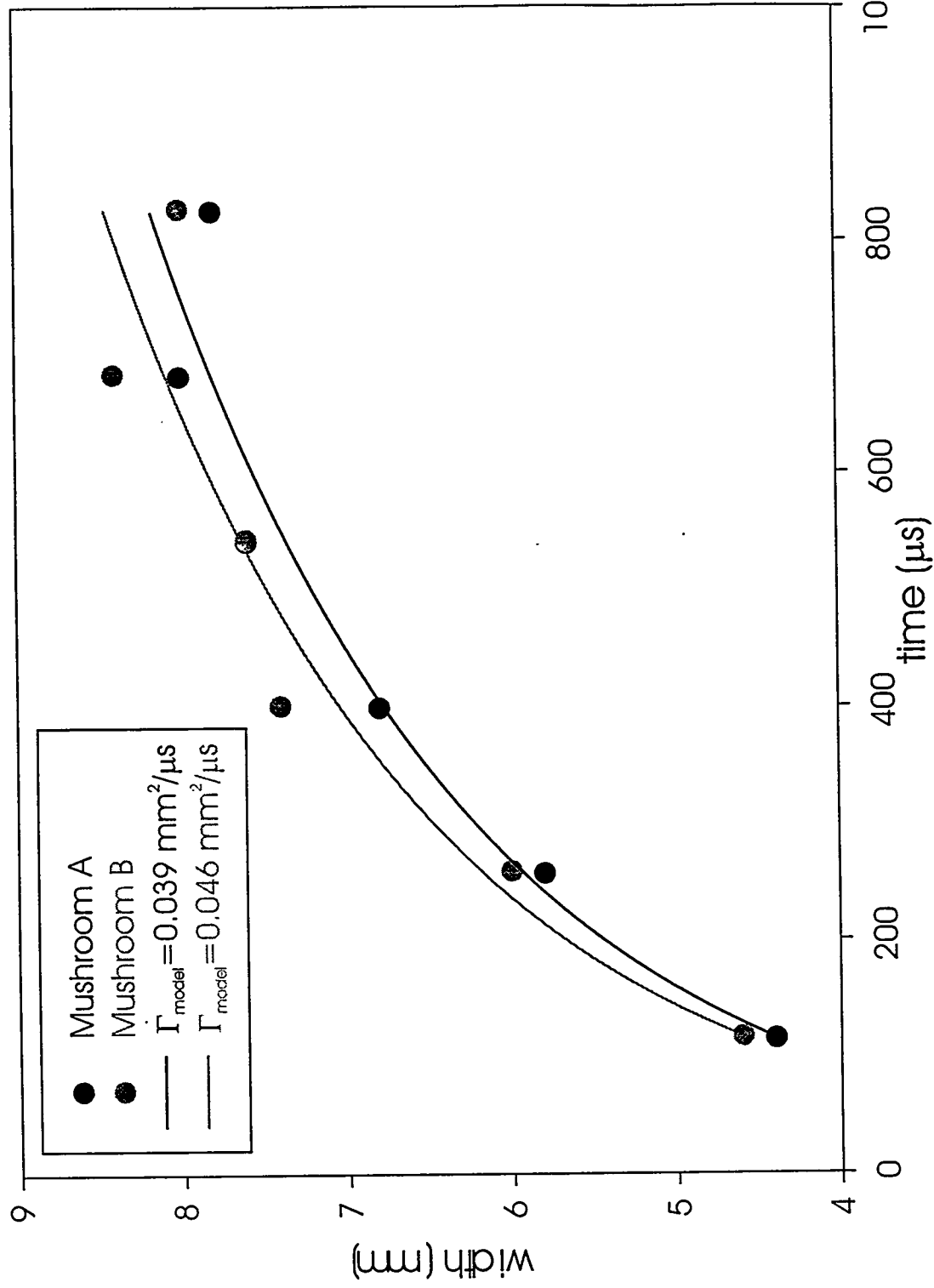
$$\Gamma_{\text{PIV}} = 0.041 \text{ mm}^2/\mu\text{s}$$



$$\Gamma_{\text{PIV}} = 0.033 \text{ mm}^2/\mu\text{s}$$

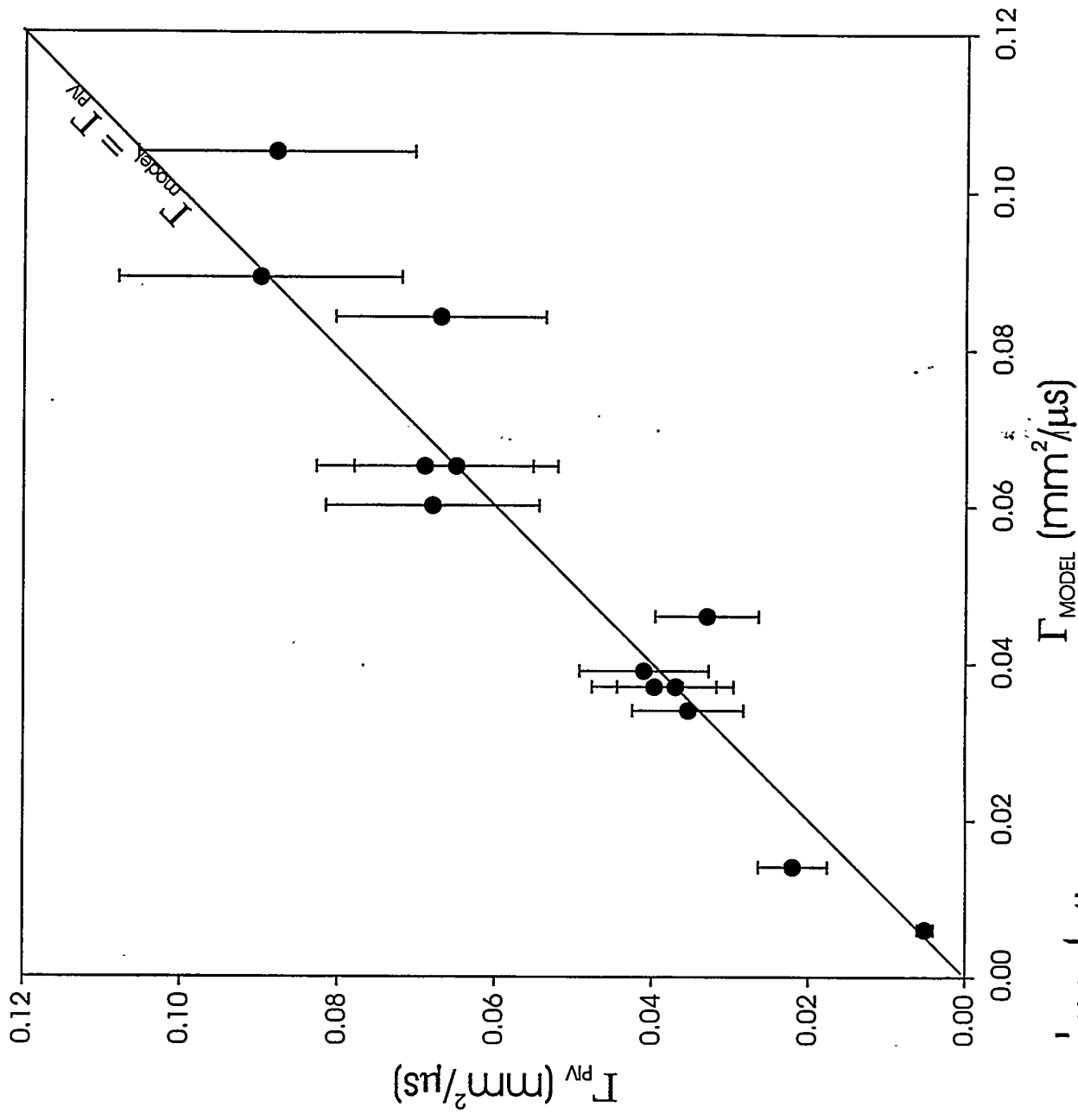


Curve fits of growth using Γ - t_0 model



From PIV measurements: $\Gamma_{\text{PIV}} = 0.041, 0.033 \text{ mm}^2/\mu\text{s}$

Comparison between Γ_{PV} and Γ_{model} for many data sets



Conclusion

We have upgraded our diagnostics to use gated CCDs and pulsed lasers, allowing us to perform simultaneous imaging and Particle Image Velocimetry (PIV).

This is the first time that PIV has been applied to a shock-accelerated fluid instability.

The velocity-field data that we have collected on the single-mode gas curtain has been used to validate a theoretical model for the growth of the curtain.